GENERAL ATOMIC

DIVISION OF GENERAL DYNAMICS

GA-4426

INTEGRAL NEUTRON THERMALIZATION

QUARTERLY PROGRESS REPORT
FOR THE PERIOD ENDING
JUNE 30, 1963

Contract AT(04-3)-167
Project Agreement No. 2
U.S. Atomic Energy Commission

July 26, 1963

DISCLAIMER

GENERAL ATOMIC

DIVISION OF

GENERAL DYNAMICS

JOHN JAY HOPKINS LABORATORY FOR PURE AND APPLIED SCIENCE

P.O. BOX 608. SAN DIEGO 12. CALIFORNIA

GA-4426

INTEGRAL NEUTRON THERMALIZATION

QUARTERLY PROGRESS REPORT
FOR THE PERIOD ENDING
JUNE 30, 1963

Contract AT(04-3)-167
Project Agreement No. 2
U.S. Atomic Energy Commission

Work done by:

J. R. Beyster
J. R. Brown
G K. Houghton
D. H. Houston
G. D. Joanou
J. Kirkbride
J. U. Koppel
Y. D. Naliboff
D. E. Parks
J. L. Russell
G. D. Trimble
J. A. Young
J. C. Young

Facsimile Price $ 4.60
Microfilm Price $ 1.64

Available from the
Office of Technical Services
Department of Commerce
Washington 25, D. C.

Report written by:

J. C. Young
J. R. Beyster
J. R. Brown
D. H. Houston
J. Kirkbride
J. U. Koppel
G. D. Trimble
J. A. Young

July 26, 1963

PREVIOUS REPORTS IN THIS SERIES

GA-2544 - Annual Report for October, 1960 through September, 1961

GA-3542 - Annual Report for October, 1961 through September, 1962

GA-3853 - Quarterly Report for October, November and December, 1962

GA-4176 - Quarterly Report for January, February and March, 1963

CONTENTS

I. INTRODUCTION

This report covers work conducted under the integral neutron thermalization program at General Atomic from April 1, 1963, to July 1, 1963, under contract AT(04-3)-167, Project Agreement No. 2, with the U.S. Atomic Energy Commission.

A strong interest in reactor systems using solid, homogeneous fuel for the SNAP application initiated a complete experimental and analytical study of the moderator zirconium hydride at various temperatures. A pre v c paper presented on this subject at the Salt Lake City American Nuclear Society meeting will be submitted to Nuclear Science and Engineering for publication in the near future. In view of the excellent agreement obtained between the thermal spectral predictions based on the Einstein oscillator model and experiment it is clear that this moderator is understood better than most and certainly adequately for all anticipated reactor applications.

Decay constant and modal analysis measurements have been completed during this quarter in the water-U^{235} critical assembly at the General Atomic electron linear accelerator facility (Linac). The measurements are presently under analysis and will be discussed in Section 2.1.

The neutron spectral measurements in poisoned water at various temperatures and pressures have been analyzed and compared with theoretical predictions. They are presented in Section 2.2.

Comparison of theoretical and experimental thermal neutron spectra for various poison concentrations of 1/v absorber (boron) in D_2O is discussed in Section 2.3.

The shielding studies conducted in conjunction with the Oak Ridge National Laboratory Neutron Physics Group are discussed in Section 2.4.

Improvements in experimental techniques for measuring spectra have continued. Comparison of the energy response of the sensitive BF_3 detector bank used in spectral studies with that of a flat response detector (Li^6 glass) for calibration purposes is discussed in Section III. Progress in the development of theoretical techniques during the quarter is discussed in Section IV.

In response to the many requests for recent experimental data and theoretical calculations, a format for presenting these data in a concise and legible form has been completed and is given in Appendix II. The example shown is that for a typical spectral experiment. Spectra in this format will be compiled for all of the best data as they become available and presented as a document for laboratory use.

A short section (Section V) on the status of the Linac facility is included to bring the reader up to date on the improvements which have been made, are now underway, and are planned for this year.

The contractual obligations for this contract year have in most part been completed, with only the feasibility studies in BeO remaining. The status of these measurements is discussed in Section 2.5. The remainder of the contract year will be spent finishing the BeO feasibility studies, analyzing the data which have been taken to date, and writing the annual report.

II. EXPERIMENTAL

2.1 CRITICAL ASSEMBLY

The Linac multiplying assembly[1] has been loaded to a critical configuration requiring 2921.5 gm of U^{235} and a core thickness of 8.64 in. The transverse assembly dimensions are 18 by 18 in. The assembly is bare and water moderated. The distinctive feature of these experiments is the geometrical setup used. The bare assembly has been moved far from any walls, floors, ceilings, or supports to eliminate room return effects. These results are less subject to ambiguity of interpretation than most so-called clean pulsed assembly data available for analysis. A total of 19 loading steps were taken in the approach to critical.

At each loading step the assembly multiplication of a steady state external neutron source was determined and an inverse multiplication vs. loading plot was used to predict the next loading. Figure 1 shows the plots of the approach to critical taken on two ion chambers and one fission counter, all external to the core. The detail of the last few loadings is shown in Fig. 2. The scatter of the last few points is apparently due to slightly different amounts of water in the region beyond the boundary in the thin dimension. This region is filled with void tanks and aluminum plates to exclude the water, but, as the loadings progress, different combinations of void tanks and aluminum plates are used.

At all except the very early loadings, the assembly was pulsed by a Linac produced, pulsed neutron source at repetition rates varying from 120 pps at early loadings to 30 pps at the last loadings. A small (1/4 in. diameter by 1/4 in. long) fission counter is positioned in a cylindrical tube, or "glory hole," which passes through the core in the thin dimension. For each pulse, the time distribution of counts is obtained from 4 μsec after the burst to a time just before the next burst, thus giving counting

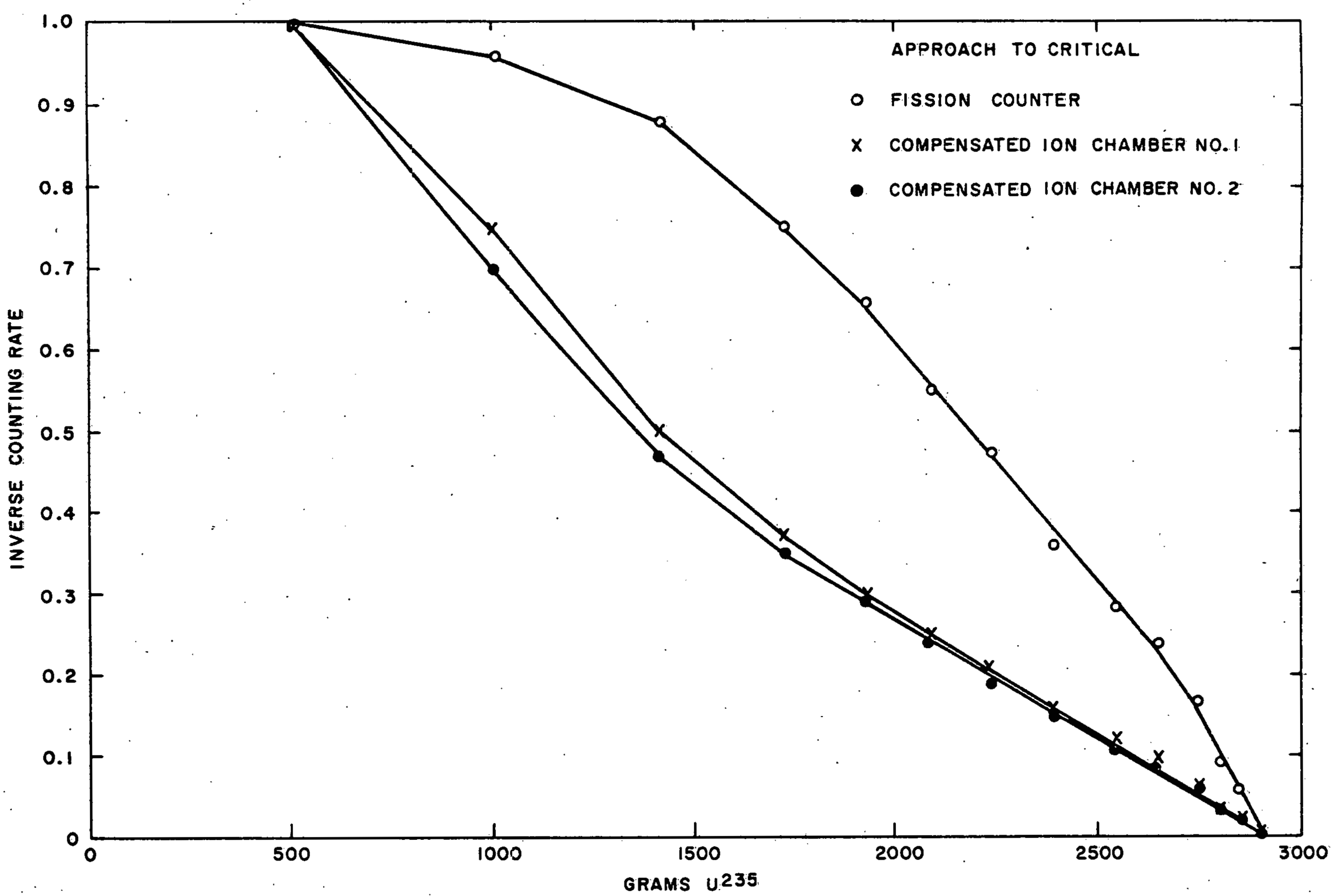

Fig. 1--Inverse multiplication curve for Linac critical assembly

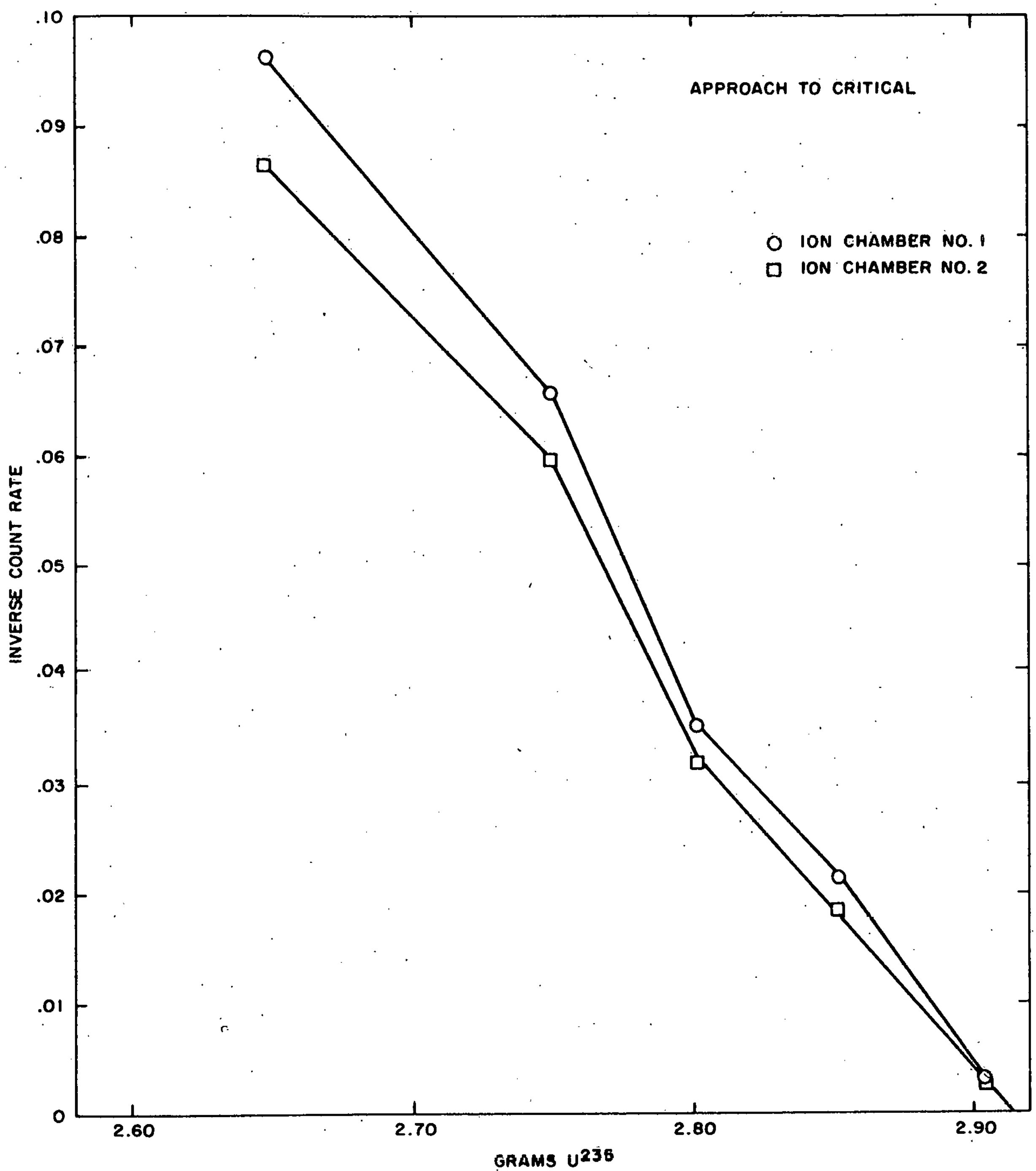

Fig. 2--Inverse multiplication curves for last few loadings of Linac critical

rates from close to zero time through the prompt die-away time region and well into the delayed neutron tail. Using these data and the method of Garelis and Russell,[2] the die-away of the fundamental mode ($1/\alpha$) and also the number of dollars the assembly is subcritical at each loading can be determined.

At three of the loadings, die-away measurements were made at each of ten positions through the thin dimension of the core, and a spatial modal analysis was performed to determine the die-away of the fundamental mode and of the next two to five harmonics. A build-up of the fundamental mode in the first 20 to 30 μsec after the burst, as previously reported[1] under less clean experimental conditions, has again been observed. A possible interpretation of this consistent result is that it is due to the decay of nonfundamental transverse modes at the early times. Figures 3, 4, and 5 show these results for the fifth, eighth, and eleventh loadings.

The results of all these measurements are in the process of analysis and will be presented in the annual report. From this analysis will come a determination of the accuracy to be expected from reactivity measurements in a simple critical or subcritical assembly using pulsed neutron techniques. Reactivity measurements by two pulsed methods and conventional techniques will be intercompared.

2.2 TEMPERATURE DEPENDENT SPECTRA IN WATER

Temperature dependent neutron spectra have been measured under infinite medium conditions in water poisoned with a 1/v absorber (boron absorption 5.15 b/H atom). The energy dependent scalar neutron flux was measured by time-of-flight techniques and the standard beam scatterer techniques, i.e., by placing a zirconium scatterer at the center of a glory hole through the

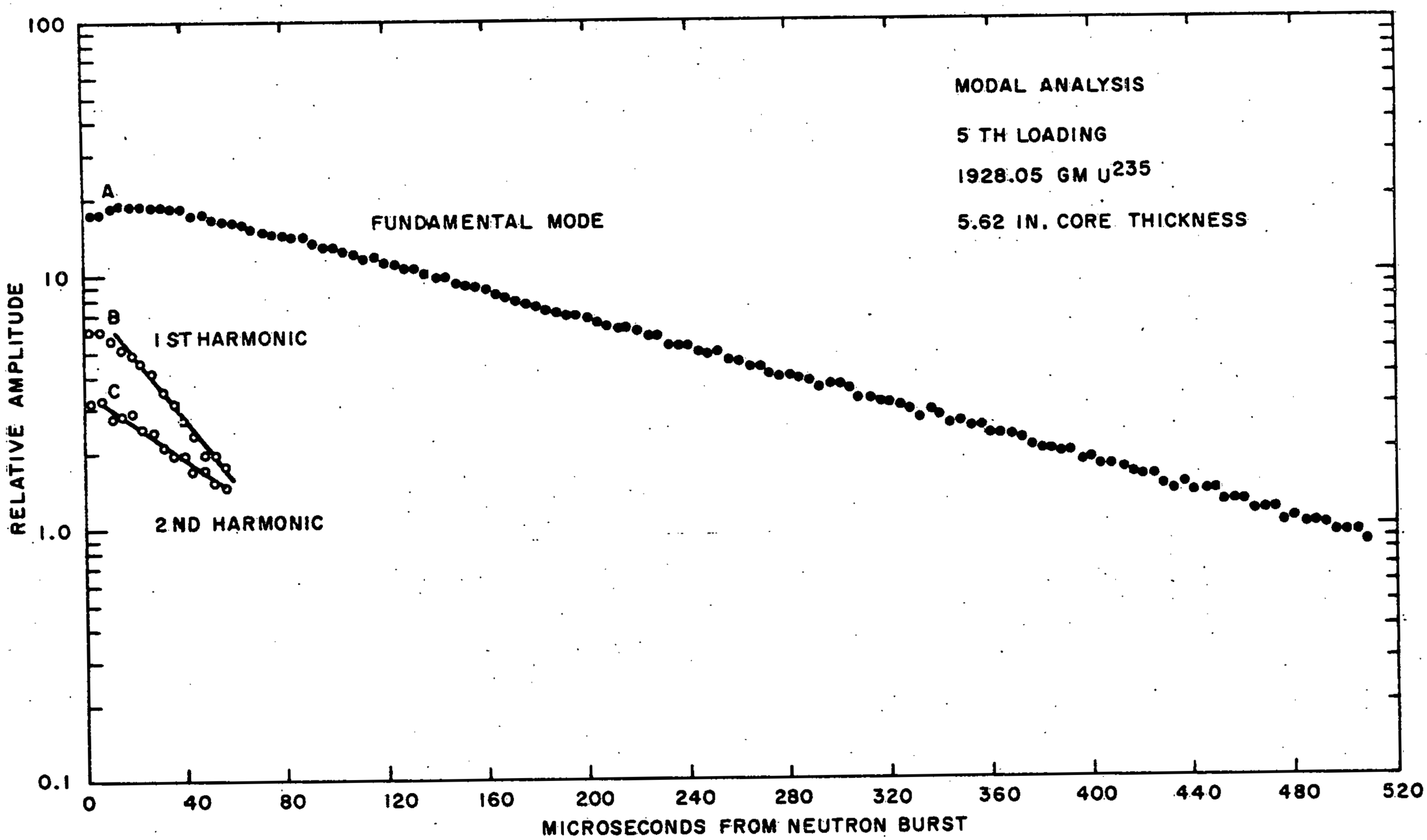

Fig. 3--Neutron density as a function of time after Linac burst at 5th loading

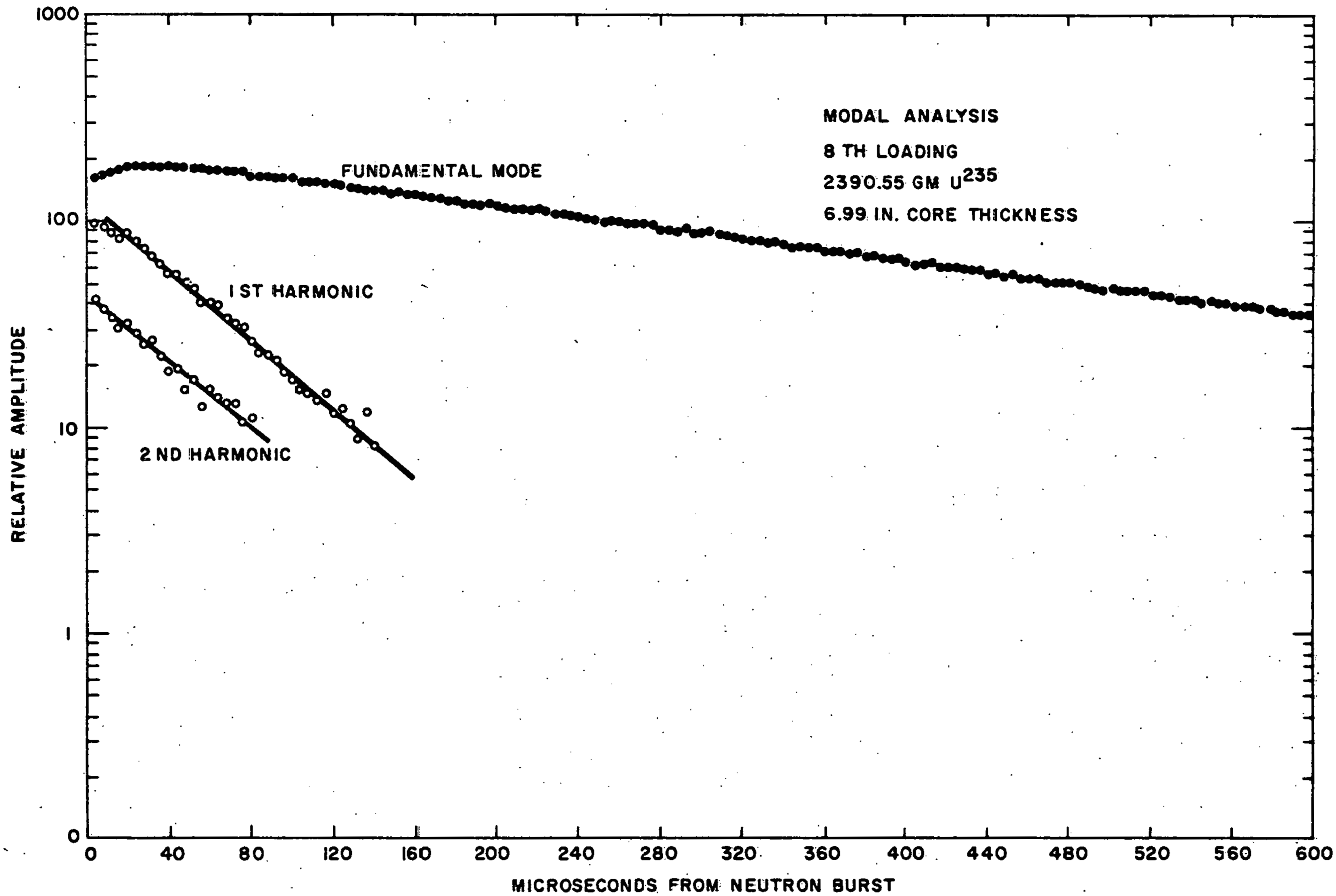

Fig. 4--Neutron density as a function of time after Linac burst at 8th loading

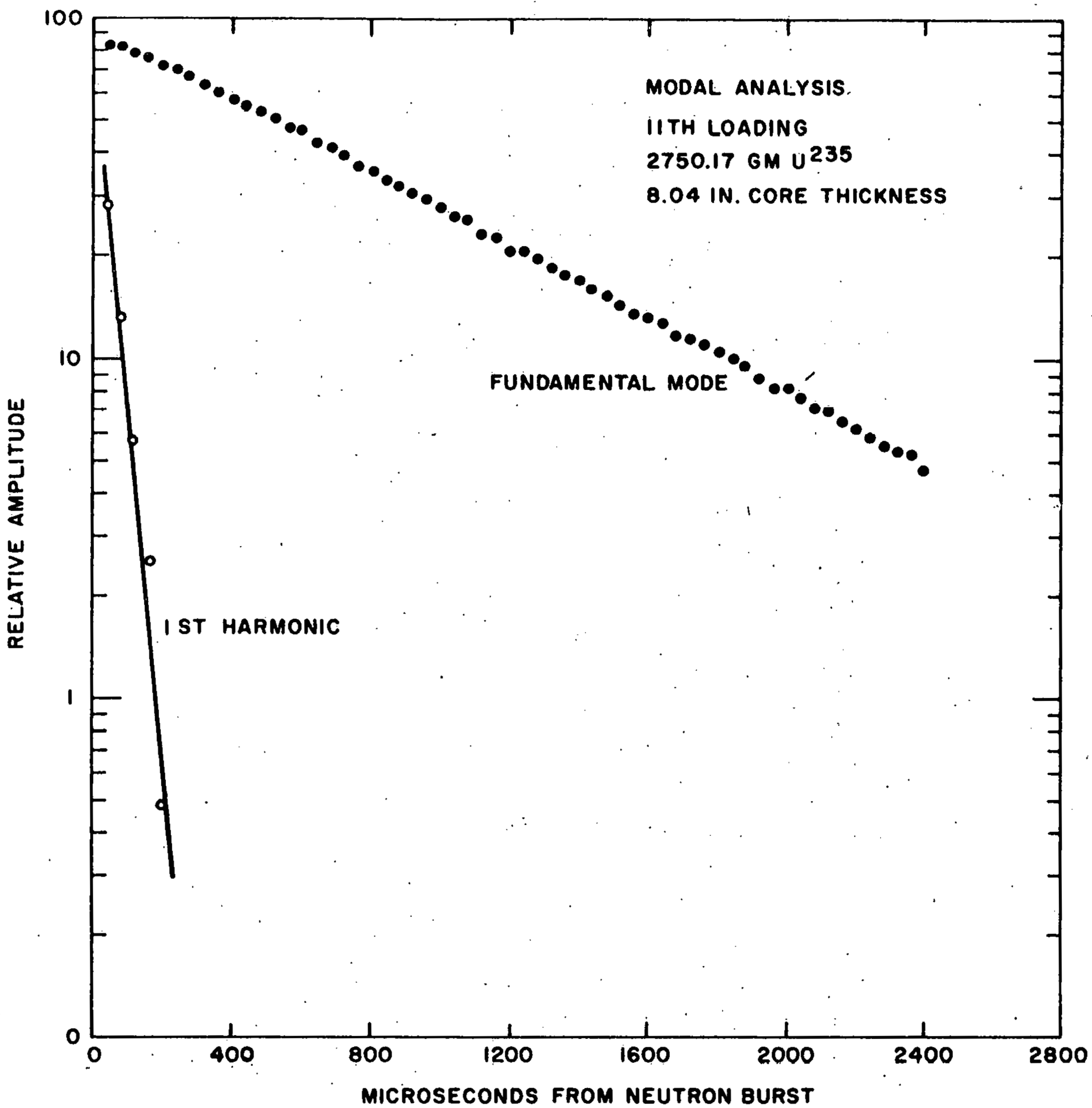

Fig. 5--Neutron density as a function of time after Linac burst at 11th loading

pressure vessel assembly. The pressure vessel was filled with 10 liters of boric acid solution and heated electrically. This vessel and the techniques for measuring spectra have been described in a previous report.[3] The measurements were performed to determine the importance of molecular binding in establishing the neutron spectrum in a high temperature water moderated reactor. Since it is known that molecular binding produces significant spectral shifts at room temperature, these spectral measurements serve to establish the magnitude and importance of the binding effects at elevated temperatures.

Infinite medium neutron spectra were measured at 30°, 150°, 232°, and 316°C. A composite curve showing the infinite medium neutron spectra at these temperatures for a homogeneously poisoned boric acid solution (5.15 b/H atom) is shown in Fig. 6. Figures 7 through 10 show the individual neutron spectrum measurements for each of the above mentioned temperatures. At each temperature a bound hydrogen theoretical claculation using Nelkin's model for water and a free hydrogen gas model are shown for comparison with the measured spectra. The small irregularity in each measured spectrum between 0.015 and 0.02 ev is thought to be due to the elastic scattering diffraction from the zirconium which was used to extract the neutron beam from the vessel to measure these spectra.

Listed in Table I are some of the salient features for these spectra. Column 1 is the temperature of the moderator is degrees centrigrade, column 2 is the temperature of the moderator in electron volts, column 3 is the neutron temperature in electron volts, and column 4 is the ratio of the two. Column 5 is the ratio of the bound hydrogen calculation of the

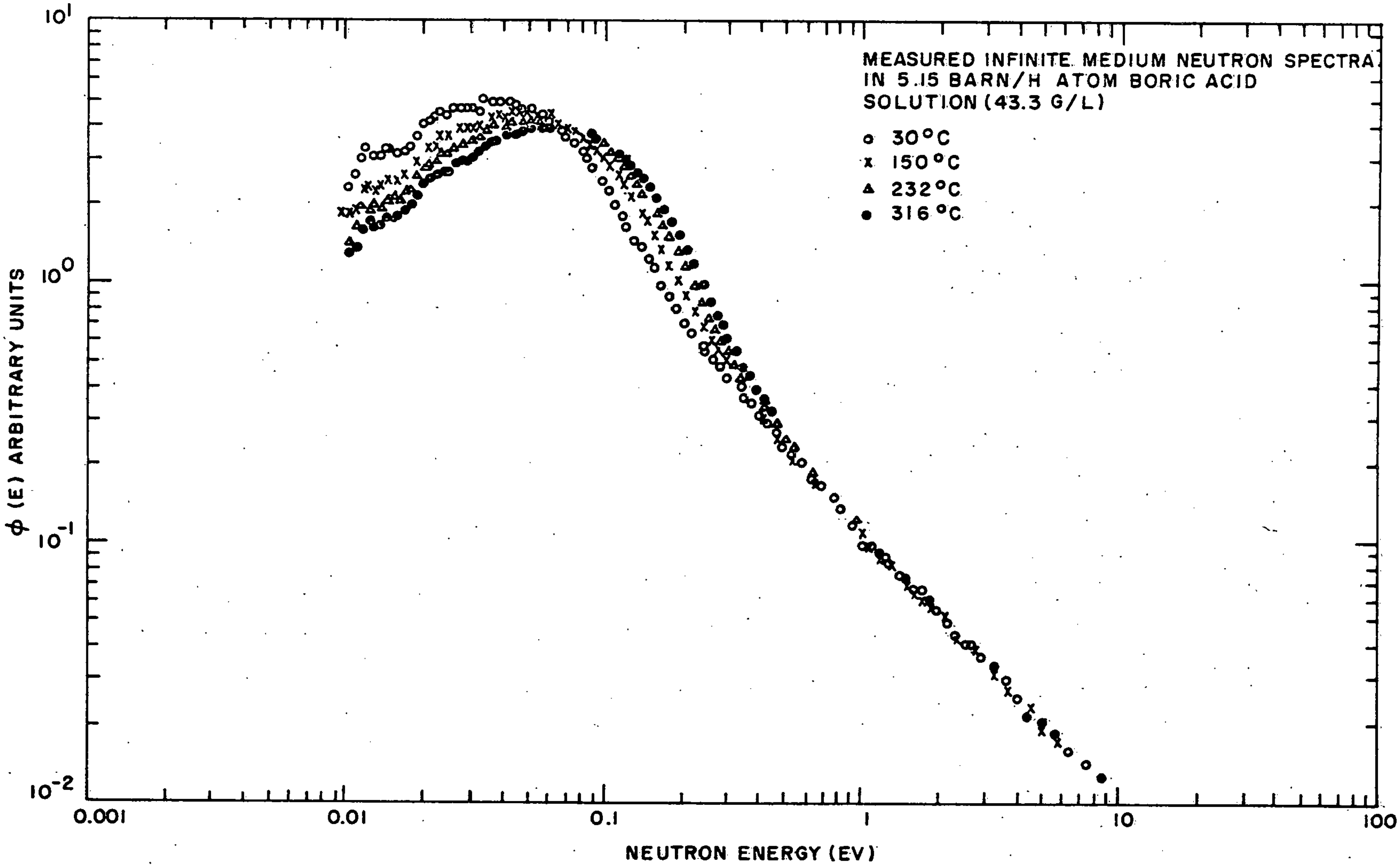

Fig. 6--Infinite medium neutron spectra in borated water as a function of moderator temperature

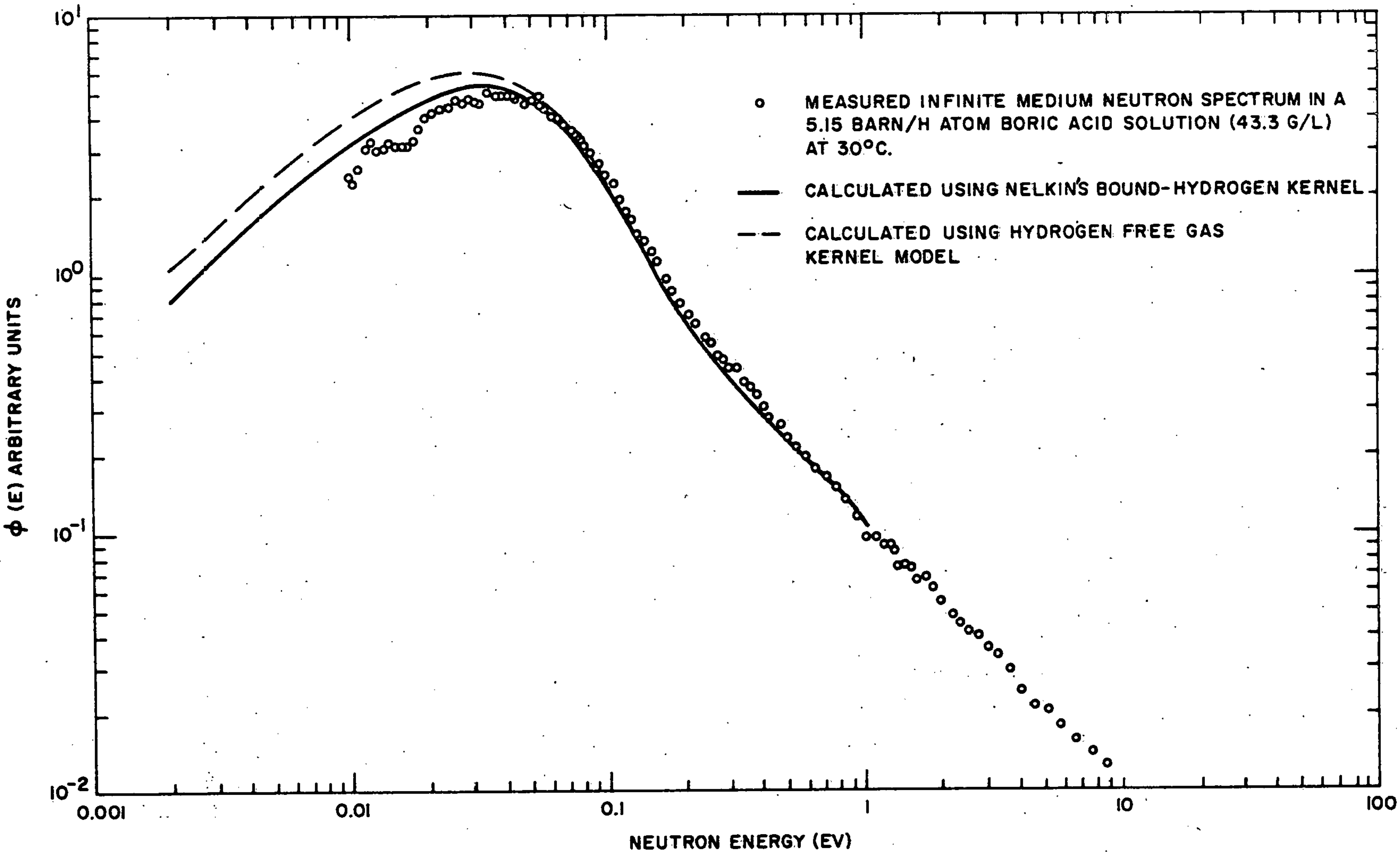

Fig. 7--Infinite medium neutron spectra in borated water at 30°C

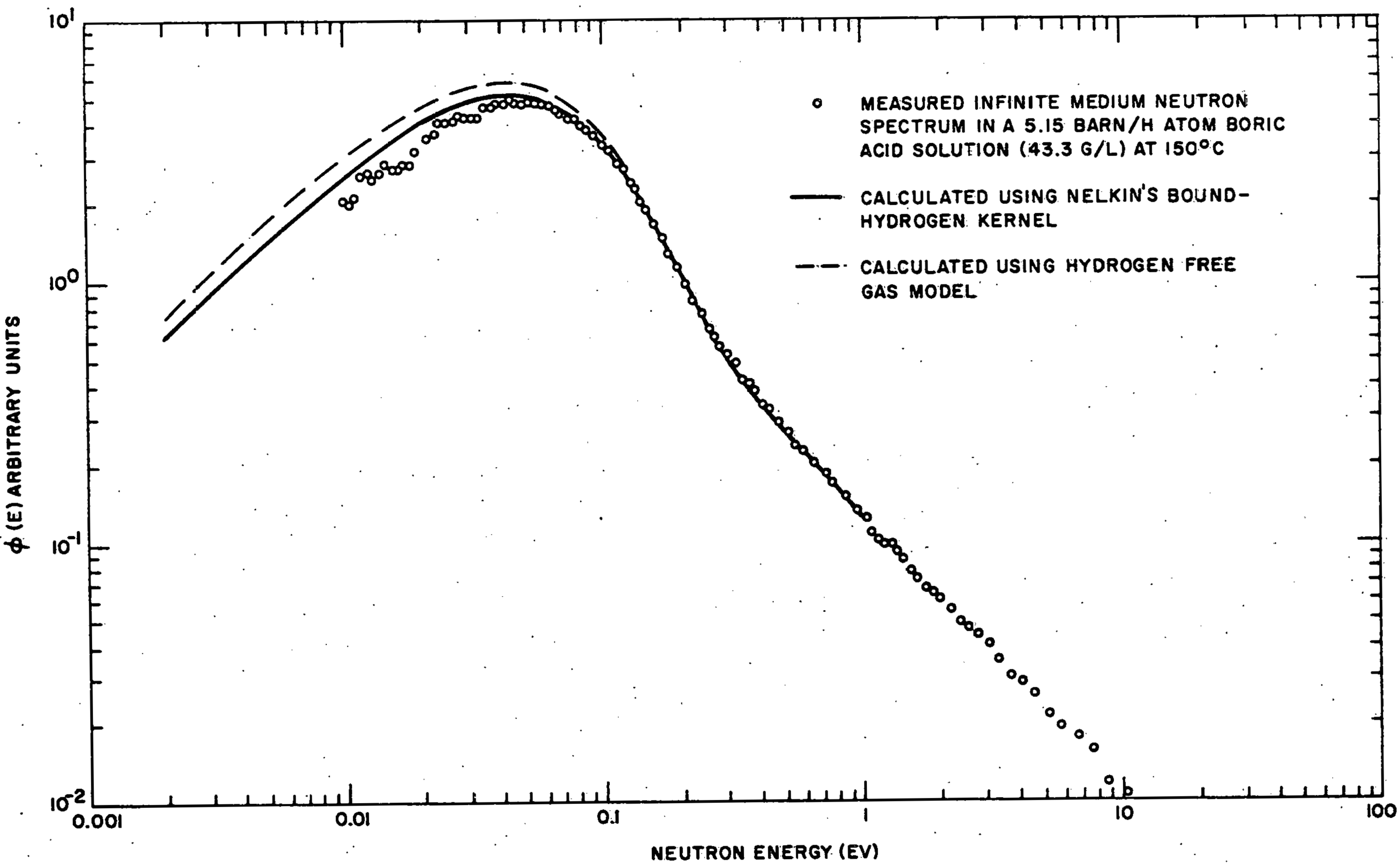

Fig. 8--Infinite medium neutron spectra in borated water at 150°C

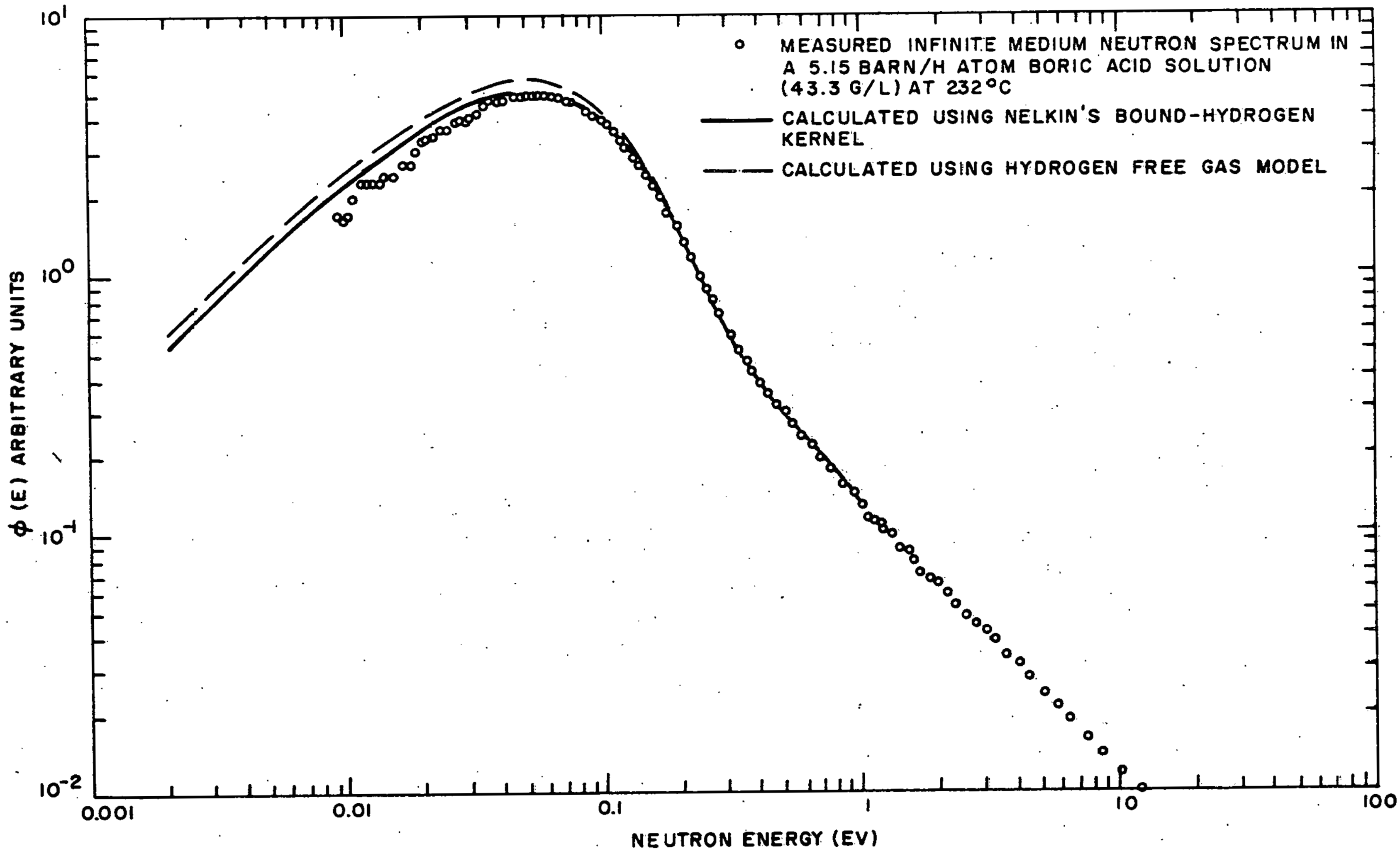

Fig. 9--Infinite medium neutron spectra in borated water at 232°C

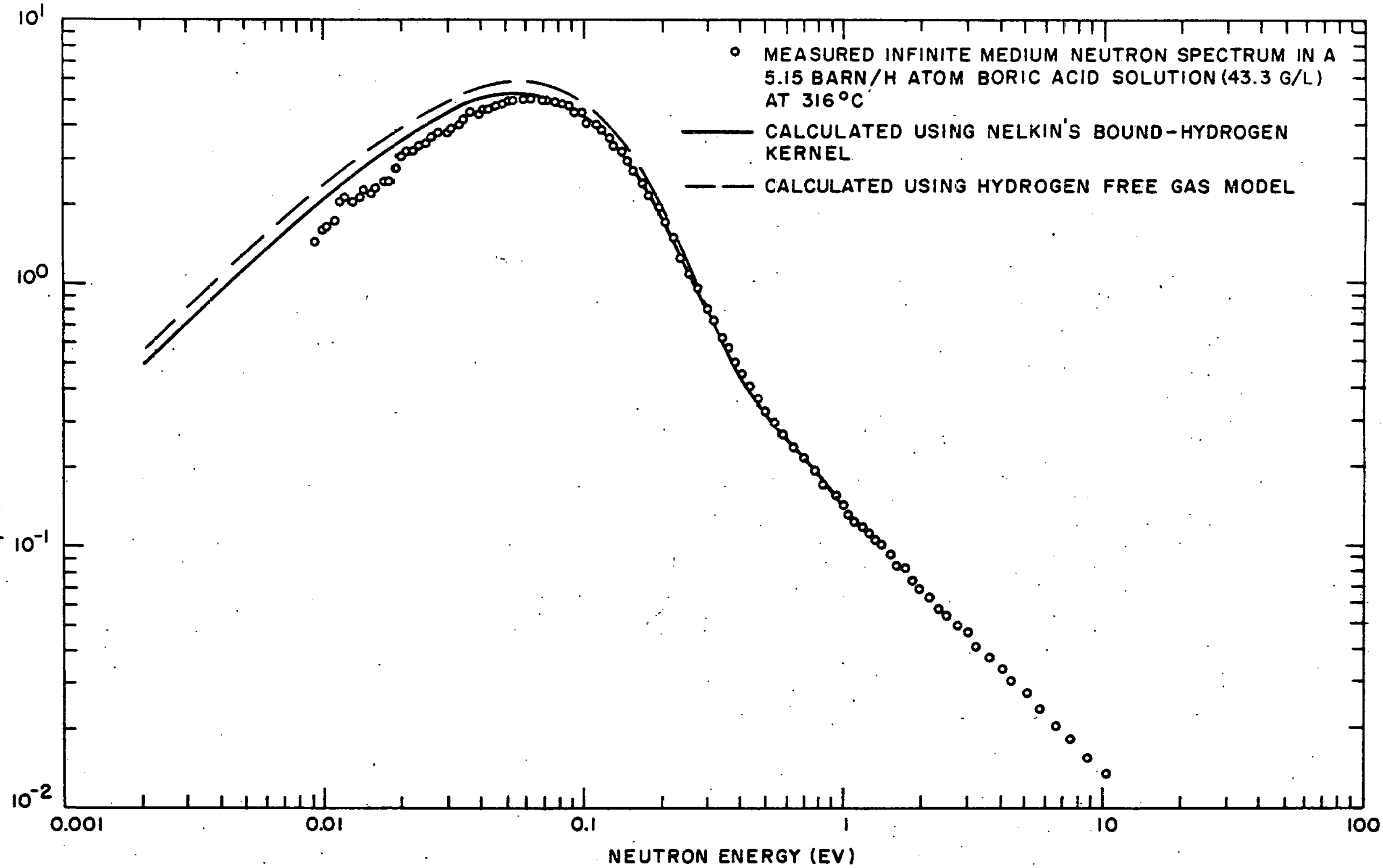

Fig. 10--Infinite medium neutron spectra in borated water at 316°C

Table I

COMPARISON OF THE THEORETICAL AND EXPERIMENTAL RESULTS

Temp. (°C)	E_M(ev)	E_N(ev)	E_N/E_M	ϕ_{BH}/ϕ_{Exp}	ϕ_{FH}/ϕ_{Exp}	ϕ_{FH}/ϕ_{BH}
30	0.0261	0.036	1.38	1.10	1.27	1.15
150	0.0364	0.043	1.29	1.09	1.24	1.14
232	0.0435	0.056	1.24	1.04	1.16	1.12
316	0.0507	0.060	1.18	1.06	1.17	1.10

spectrum to the measured spectrum at KT and column 6 is the ratio of the free hydrogen calculation of the spectrum to the measured spectrum. Column 7 is the ratio of the calculated free hydrogen flux to the calculated bound hydrogen flux. The theoretical and experimental spectra were normalized at 1 ev for comparison and the ratio of the fluxes were compared at E_M, the moderator temperature.

It can be seen in Table I that the bound hydrogen description is adequate for describing the neutron scattering processes in water at a temperature of 316°C and that the free hydrogen calculation does not give as accurate a description of the observed spectrum in water. This comparison illustrates the fact that molecular binding is still important at operating temperatures for water-moderated reactors and that the free hydrogen model is not appropriate for reactor calculations at these temperatures.

Another qualitative feature of these temperature dependent spectra is the lack of a marked change in the spectral shape as one increases the temperature of the moderator through 150°C. Results reported in Table I and Figs. 7 through 10 are thus not consistent with Egelstaff's suggestion that model parameters need to be adjusted in going from 23°C to 300°C. Further experiments at elevated temperatures to investigate resonance absorption effects on spectra will be conducted later this year with a mixture of the absorbers gadolinium or samarium and erbium. This should complete the infinite medium spectral studies in water, since sufficiently accurate information is available for validation of the molecular model refinements now underway at General Atomic.

While infinite medium neutron spectra in water moderated systems are reasonably well understood for most reactor applications, spectra of angular flux are not as yet. It will be recalled that a thorough series of angular flux measurements[4] has been completed in poisoned and unpoisoned water slabs and the comparisons with theory have not been encouraging. One mechanism which was postulated to explain the discrepancy was that the experimental high energy neutron source distribution might influence the measured thermal angular flux. Experimentally this idea was investigated by relocating the external sources in an entirely different way.[3] The thin slab measurements still were not affected much by this change. Analytically we have calculated the entire fast-slow flux problem, including the external source, with the transport code DSN. The problem was broken into two pieces: the fast problem ($E > 1.4$ ev) and the thermal problem ($E < 1.4$ ev). In the fast problem the source placement was included, the actual slab water geometry was specified, 17 energy groups were used, and S_{16} transport approximations and P_3 elastic scattering were utilized. The source for the thermal problem (with upscattering) was calculated in the ev region. Actually, three energy groups were used below 10 ev. It turned out that the spatial and angular flux distributions were very similar for all three "source" groups but that these distributions differed strongly from the diffusion theory (P_1) spatial and angular sources used in the previous analysis. It appears that the angular flux distribution, even at energies of a few ev, maintains a strong memory of the incident fast neutron direction. All of this looked hopeful, but the thermal flux DSN results obtained with the new angular sources were not significantly different from those obtained in previous calculations. For the thermal problem 23 energy groups and 60 spatial mesh points were used. Thus, the method of experimental analysis has been refined to about the limit, and the reason for discrepancies in angular fluxes must be in the input data, especially the scattering levels for water. Measurements of scattering angular distribution, $\sigma(E,\mu)$, to be reperformed more precisely in water during this next quarter, should go a long way toward settling this problem. In the theory section of this report (Section IV) the present effects underway to generate a more physically realistic kernel for water are also discussed. These two undertakings should provide sufficient information to resolve the angular flux paradox.

2.3 NEUTRON SPECTRA IN BORATED D_2O

The previously reported[4] infinite medium spectral studies in D_2O containing 3.6% light water were repeated[3] using pure D_2O. As reported previously[4] the attempts to fit these data using current scattering kernels were only moderately successful. In the earlier measurements the free gas scattering matrix yielded a better fit to the experimental data than did the more realistic bound deuterium kernel of H. Honeck, which is patterned after Nelkin's model for light water. This quarter the calculational effort for the moderator D_2O was directed toward generating a Nelkin type scattering kernel with a higher maximum thermal cutoff energy than the 0.7 ev used previously. This will make it possible to more accurately normalize the calculations with experiment in the slowing down region.

The results of the theoretical calculations of the scattering matrix with a 2 ev thermal cutoff energy are not yet complete. These calculations should be completed in the near future and will be reported in the annual report.

2.4 SHIELDING STUDIES

These measurements were performed in close collaboration with Dr. V. Verbinski of Oak Ridge National Laboratory, who designed the shields and experimental geometries. After a particular shield configuration had been selected and set up in the Linac low background cave, the penetration neutron spectrum was measured, first with Verbinski's detection equipment and afterwards under identical conditions with the General Atomic fast neutron detection equipment. This produced two independent sets of spectral data. The General Atomic equipment and techniques are discussed below.

For neutrons with energies in excess of 100 kev, the most efficient detector is the organic scintillator, from which recoil-proton scintillations can be analyzed. Since Verbinski had previously selected the Forté method of pulse shape discrimination for rejection of gamma scintillations, we adopted the Owen-Batchelor method.[5,6] This involved the special design of discriminator and coincidence circuits. In the pilot experiments it became clear that in the time interval 1.0 to 10 μsec after the Linac burst there were very few gamma scintillations compared with neutron scintillations. By placing a gamma filter of 2 in. of lead across the beam at the 16 meter position, virtually all gammas were removed while 30% to 40% of neutrons were transmitted. At the 32 meter position a thick wax and lead wall was constructed with an 8 by 8 in. aperture for the beam. Finally, at 50 meters the 2 by 2-1/2 in. scintillator was placed in the center of the 12 by 12 in. beam. Initially many pilot runs were made at low Linac intensities in order to examine the neutron to gamma ratios. Later high intensity runs were made in which pulse shape discrimination was omitted and replaced by transmission tests. Two transmission samples which were used are listed in Table II.

Table II

SAMPLE TRANSMISSIONS

Sample	Thickness	Gammas	Fast Neutrons
Pb	60 gms/cm^2	< 9%	30% to 40%
CH_2	7 gms/cm^2	> 70%	40% at 10 Mev 4% at 1 Mev

The neutron transmissions of these samples from 0.5 Mev to 15 Mev agreed with the calculated transmissions to within statistics ($\pm$ 6%). The presence of gammas in the scintillation spectra would have caused a low value for lead and a high value for the polyethylene transmission. The results to date indicate that there is less than 5% gamma contamination in the fast neutron flux for all experimental shielding configurations. This transmission test was repeated with a 20 cm water shield in the beam at the cave, and similar results were obtained. Since the gamma contamination was lower than 5%, it was decided to omit pulse shape discrimination; this permitted the Linac intensity to be increased by a factor of more than ten, giving much shorter run times.

The water shield experiments performed are listed in Table III.

Table III

WATER SHIELD EXPERIMENTS

Water Thickness (cm)	Angle of Emergence Large Target, 8x8x8 in.	Small Target, 3/4x2 in. dia.
0	0	
10	30°	
20	0, 30°	
30	30°	0°, 1°, 2°
40	0	

The water shields were extended by boxes of wax to form an approximate half sphere around the large target. This gave a geometry compatible with the NIOBE code.

One salient feature of the shielding results was the effect of the oxygen resonance at 3.5 Mev even for a relatively thick shield. This is illustrated by the data at 0° shown in Fig. 11.

2.5 BeO FEASIBILITY STUDIES

These studies are being made to determine the feasibility of obtaining a three dimensional normal mode flux distribution in a BeO assembly. An X-ray source and the (γ,n) reaction in the beryllium itself are utilized to shape the spatial distribution of the fast flux. If the technique works, it may obviate the need for multiplying assembly studies of spectra for this moderator. The availability and size of the BeO blocks to be used limit the design of the assembly. From the materials available, an assembly 60 by 60 by 60 cm has been stacked from blocks about 1 cm thick. Each layer of BeO is poisoned with 0.010 in. thick borated stainless steel. This will give a poison concentration of about 1.3 barns per beryllium

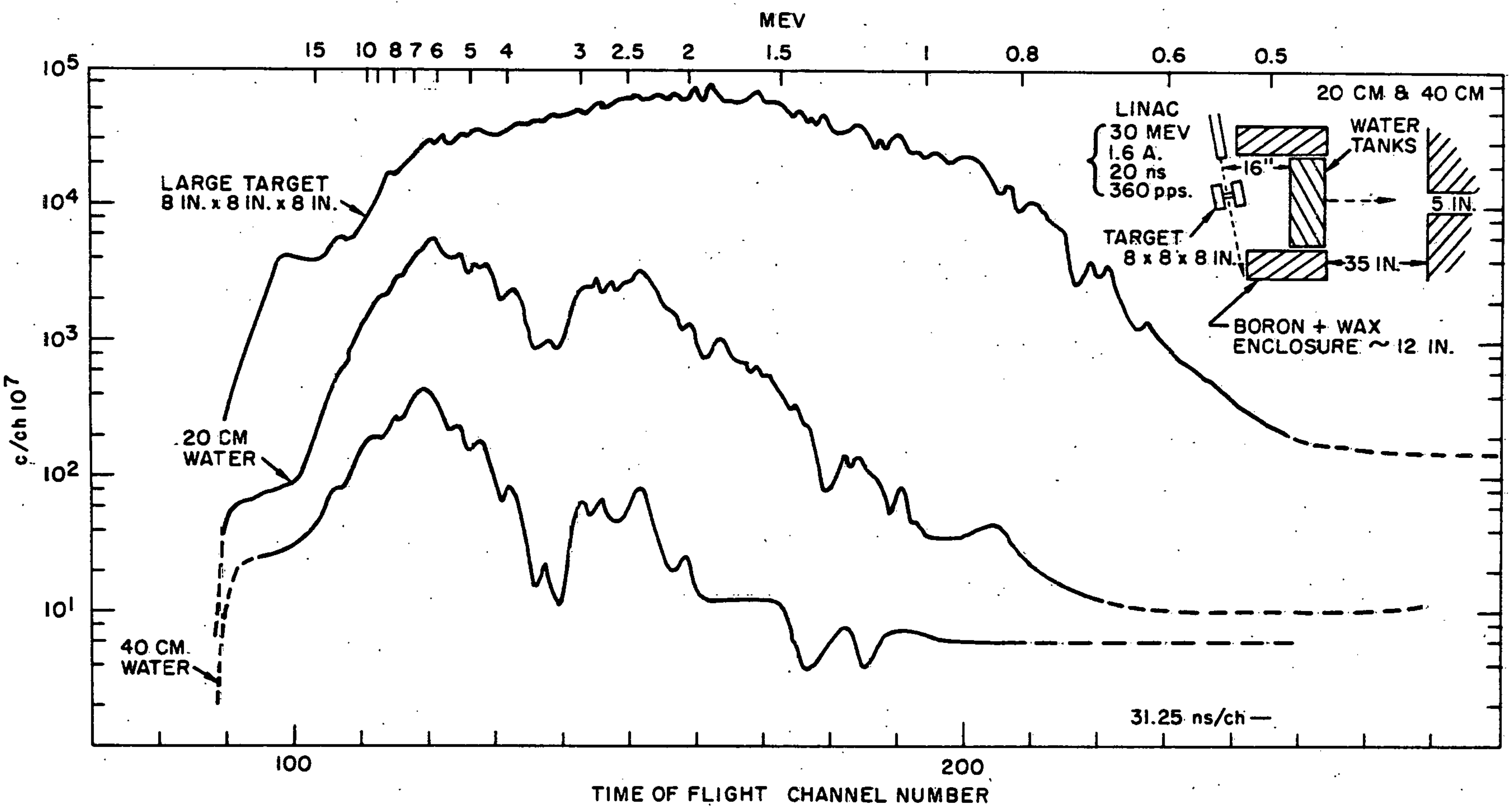

Fig. 11--Thick water shield neutron penetration spectra (0° direction)

atom and a negligible self absorption correction. Since $\Sigma_a/\xi\ \Sigma_s = 0.75$, the spectrum will be quite hard but still should be sensitive to the scattering model. The X-ray source to be used is constructed of 0.020 in. tungsten alloy to convert the Linac electron beam to a thick target X-ray spectrum. The target is water cooled and is backed by 2 in. of aluminum to stop the remaining electrons. The assembly will be pulsed and the neutron flux distributions mapped using cadmium covered indium foils. The geometrical arrangement to be used is shown in Fig. 12.

A calculation of the fast neutron generation rate in the BeO has been done to determine a trial placement of beryllium blocks in the source hole.

It is anticipated that the desired cosine distributions can be obtained (empirically) by moving the source or changing the distribution of thicknesses of the BeO filler blocks shown in Fig. 12.

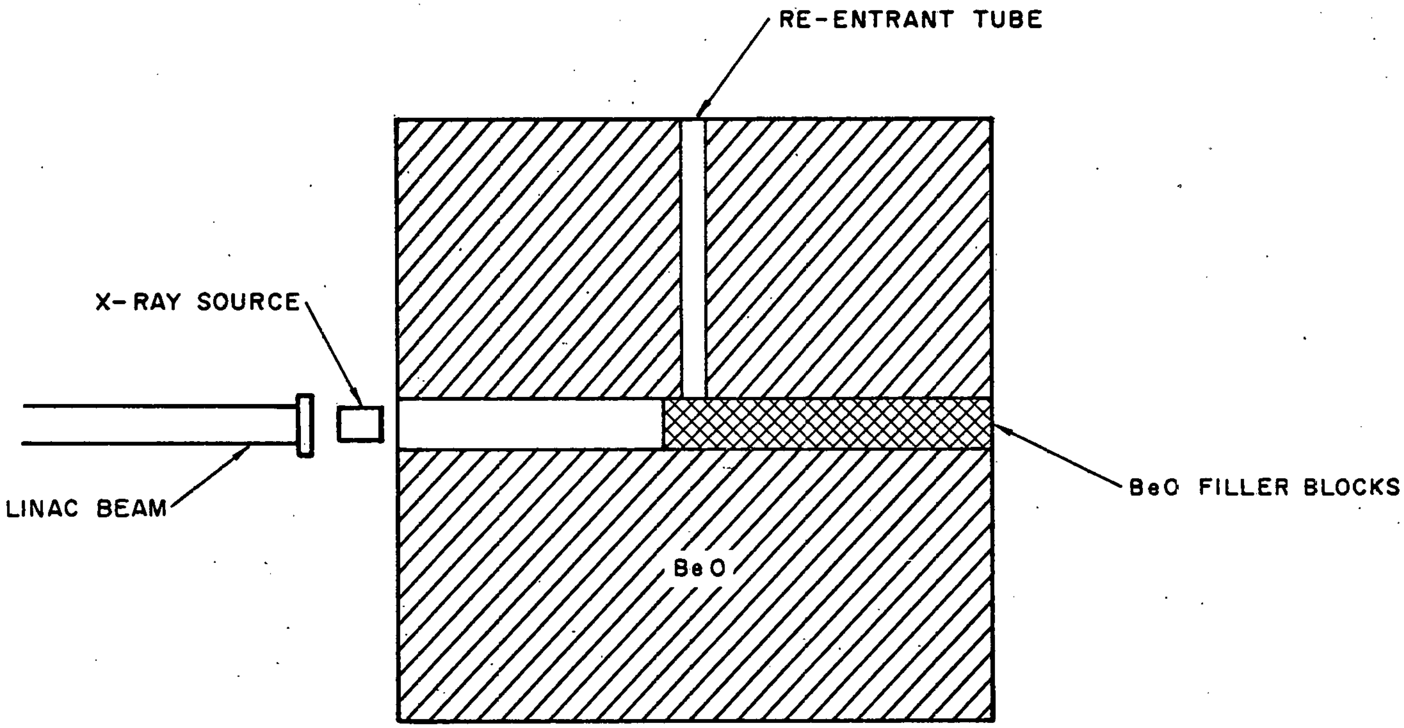

Fig. 12--Geometrical arrangement used for BeO feasibility studies

III. IMPROVEMENT IN EXPERIMENTAL TECHNIQUES

One of the most important corrections to the experimental data needed to obtain neutron spectra is the energy dependent detector sensitivity. This quantity has been measured previously by comparing the results from the sensitive BF_3 detector bank, which is used to measure spectra, with those from a thin 1/v detector. To improve the accuracy of this measurement and to check its validity in a manner independent of the 1/v detector, a comparison was made, for a standard spectrum, of the BF_3 bank spectra and of that measured by a flat response detector. A Li^6 glass scintillator was used for this comparison. The calculated efficiency of the Li^6 detector showed it to be flat to within a few percent up to about 1 ev neutron energy. Preliminary reduction of the comparison between the two detectors indicates that the sensitivity of the BF_3 bank may be lower than previously believed at low neutron energies (< 0.02 ev). The first series of measurements was made with an alpha-alumina reflector on the Li^6 glass. It is possible that this may have suppressed the neutron flux at low energies, thus accounting for the discrepancy between the sensitivities measured with the 1/v detector and the Li^6 detector. To check this point, the alpha-alumina reflector was removed and the measurements were repeated. These measurements are presently being analyzed.

IV. THEORY

4.1 ZIRCONIUM HYDRIDE

The work reported here is an extension of the theoretical analysis for zirconium hydride reported in Appendix I. In order to obtain closer agreement between theory and experimental neutron spectral results for zirconium hydride, the effects of the acoustic vibrational modes were included in the usual calculation of the scattering kernel. The optical mode was treated in the usual manner, with $h\nu = 0.13$ ev, and a natural level width. The effective mass attributed to the acoustic modes was at first taken to be 91 (the mass of one zirconium atom). This choice smoothed out the bumps due to the optical mode in the theoretical neutron spectrum at higher neutron energies, but at low neutron energies, below 0.03 ev, the agreement with experiment was not satisfactory. As a second choice, a mass of 360 was associated with the acoustic modes, resulting in very good agreement with experiment over the whole spectrum. The spectra are shown in Fig. 13, which compares the theoretical neutron spectra in $ZrH_{1.7}$, using masses of 360 and infinity for the acoustic modes, with the experimental points.

4.2 BERYLLIUM

In order to investigate neutron thermalization in beryllium it is necessary to formulate a reasonable physical model of the lattice structure of the metal. Beryllium has the hexagonal close-packed lattice structure, and in the harmonic approximation, under the assumption of central forces, the lattice vibrations are described by the equation

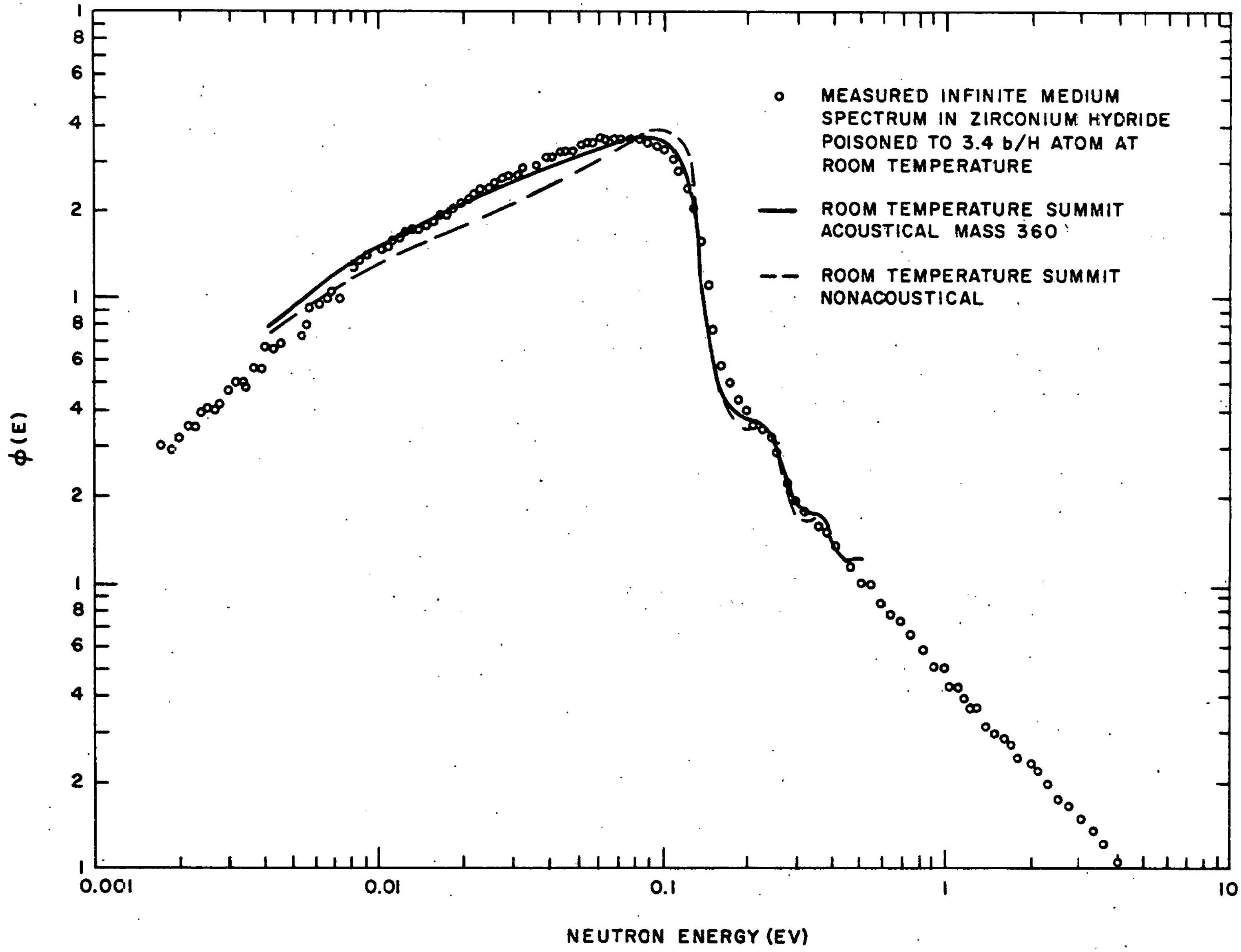

Fig. 13--Infinite medium neutron spectra in zirconium hydride at room temperature

$$M \ddot{\vec{u}}(\ell, j) = \sum_{\ell', j'} K(\ell\ell', jj') \frac{\vec{s}_o(\ell\ell', jj') \left\{ \vec{s}_o(\ell\ell', jj') \cdot \left[\vec{u}(\ell', j') - \vec{u}(\ell, j) \right] \right\}}{s_o^2(\ell\ell', jj')}$$

where $\vec{u}(\ell, j)$ is the displacement of an atom from its equilibrium position, $\vec{s}_o = x(\ell, j) - \vec{x}(\ell', j')$ are the equilibrium separations of the atoms, M is the mass of a beryllium atom, $K(\ell\ell', jj')$ are the force constants which depend only on the equilibrium separations of the atoms, and ℓ, j are the lattice and all indices, respectively. Assuming the plane wave solutions

$$\vec{u}(\ell, j) = \vec{\omega}(j)\ e^{2\pi i \left[\vec{k} \cdot \vec{x}(\ell) - \nu t \right]},$$

leads to the condition for solubility

$$\left| D_{\alpha\beta}\left(\begin{smallmatrix}\vec{k} \\ jj'\end{smallmatrix}\right) - 4\pi^2 M\nu^2(\vec{k})\ \delta_{\alpha\beta}\delta_{jj'} \right| = 0 \qquad (1)$$

where $D_{\alpha\beta}\left(\begin{smallmatrix}\vec{k} \\ jj'\end{smallmatrix}\right)$, the dynamical matrix, is given by

$$D_{\alpha}\left(\begin{smallmatrix}\vec{k} \\ jj'\end{smallmatrix}\right) = -\sum_{\ell'} K(\ell\ell', jj') \frac{s_{o\alpha}(\ell\ell', jj') s_{o\beta}(\ell\ell', jj')}{s_o^2(\ell\ell', jj')}\ e^{2\pi i \vec{k} \cdot \left[\vec{x}(\ell') - x(\ell) \right]}$$

$$+ \delta_{jj'} \sum_{\ell', j''} K(\ell\ell', jj'') \frac{s_{o\alpha}(\ell\ell', jj'') s_{o\beta}(\ell\ell', jj'')}{s_o^2(\ell\ell', jj'')}$$

Because of the periodicity of the lattice, $\vec{k}$, the wave-vector can be restricted to one Brillouin zone. In order to determine the frequency spectrum of beryllium we solve Eq. (1) for ν for various values of $\vec{k}$ in the first Brillouin zone. A histogram is then constructed for the values of ω and this yields the frequency spectrum.

The values of the force constants $K(\ell\ell', jj)$ have been determined by Schmunk, et al.[7] under the assumption of central forces with up to fifth nearest neighbor interactions. The dispersion relations in the symmetry directions of the crystal calculated on the basis of this model agree very well with experiment.

Once the frequency spectrum has been obtained in this way, the computer code SUMMIT[8] can be used to generate a scattering kernel for beryllium. Also the frequency spectrum of the crystal can be compared with the scattering law measurements of Egelstaff, and will provide a good test on how well crystal frequency spectra can be inferred from his measurements.

The work described above is very near completion, and a preliminary curve of the frequency spectrum of beryllium is shown in Fig. 14. After the theoretical work has been brought to a reasonable point so that comparisons can be made with experiment, the far more complex problem of generating a physically realistic trial scattering kernel for BeO will be attempted.

4.3 LIGHT WATER

For neutron thermalization in water, the code GAKER has been modified in order to account for the anisotropy of the different harmonic oscillators, as described in the last quarterly report.[3] Preliminary results seem to indicate that the influence of the anisotropy of the P_o and P_1 matrices is not at all negligible. This is seen in Figs. 15 through 18.

The solid line corresponds to the standard isotropic kernel calculated for 55 energies. The crosses represent a few points obtained for the

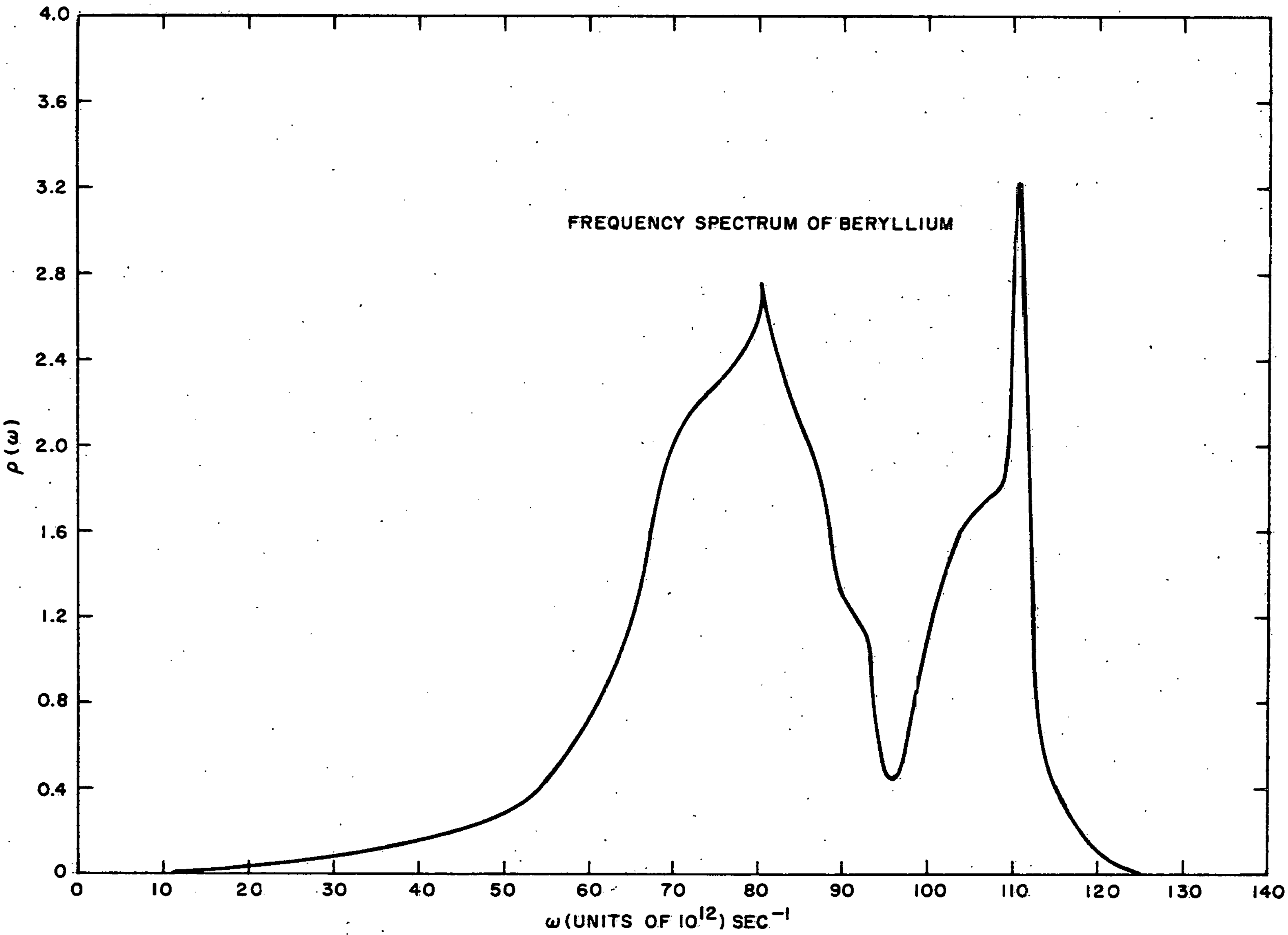

Fig. 14--Frequency spectrum of beryllium

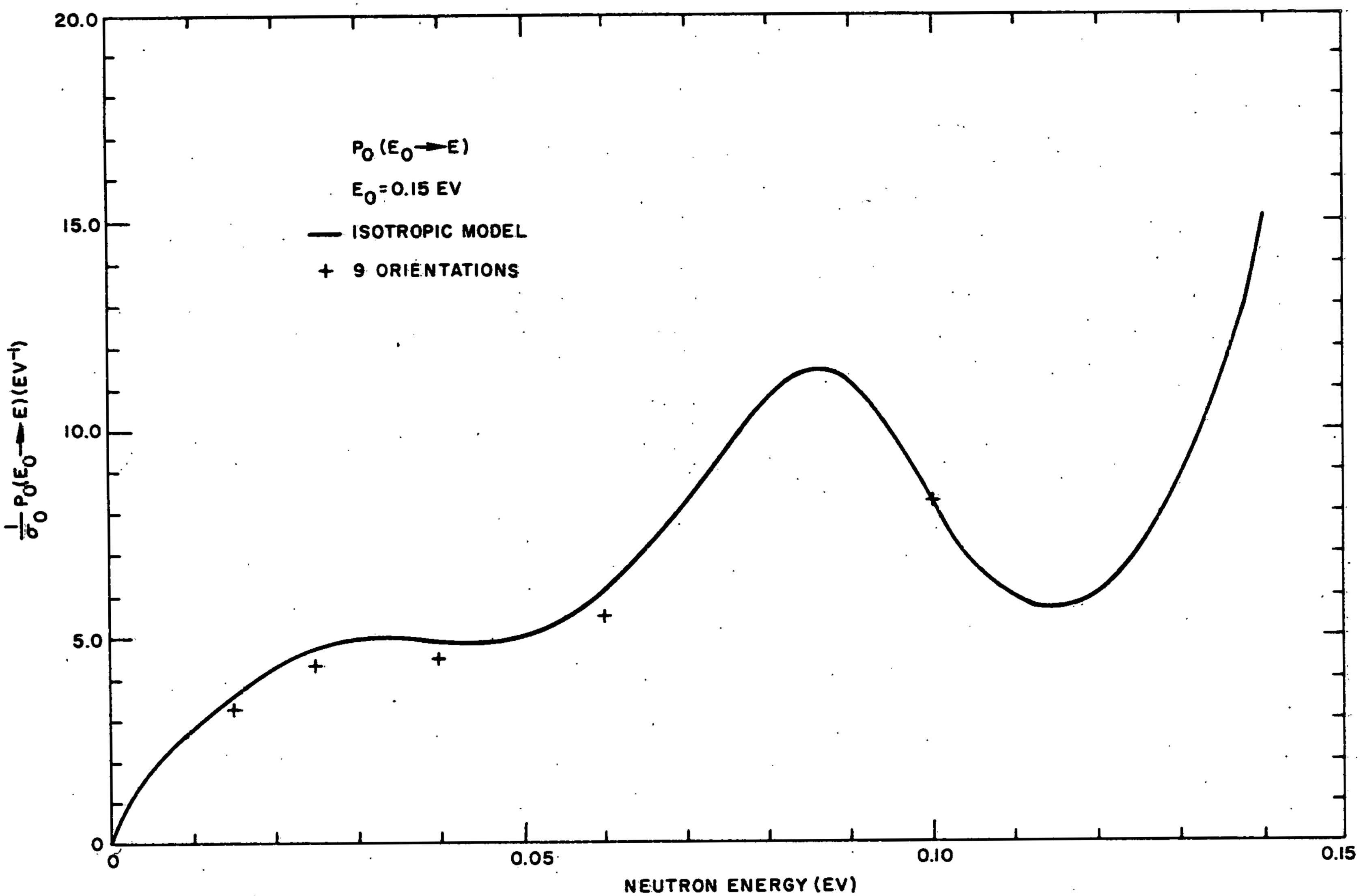

Fig. 15--Comparison of isotropic and anisotropic model for neutron scattering by water: $P_o(E_o \rightarrow E)$ at $E_o = 0.15$ ev

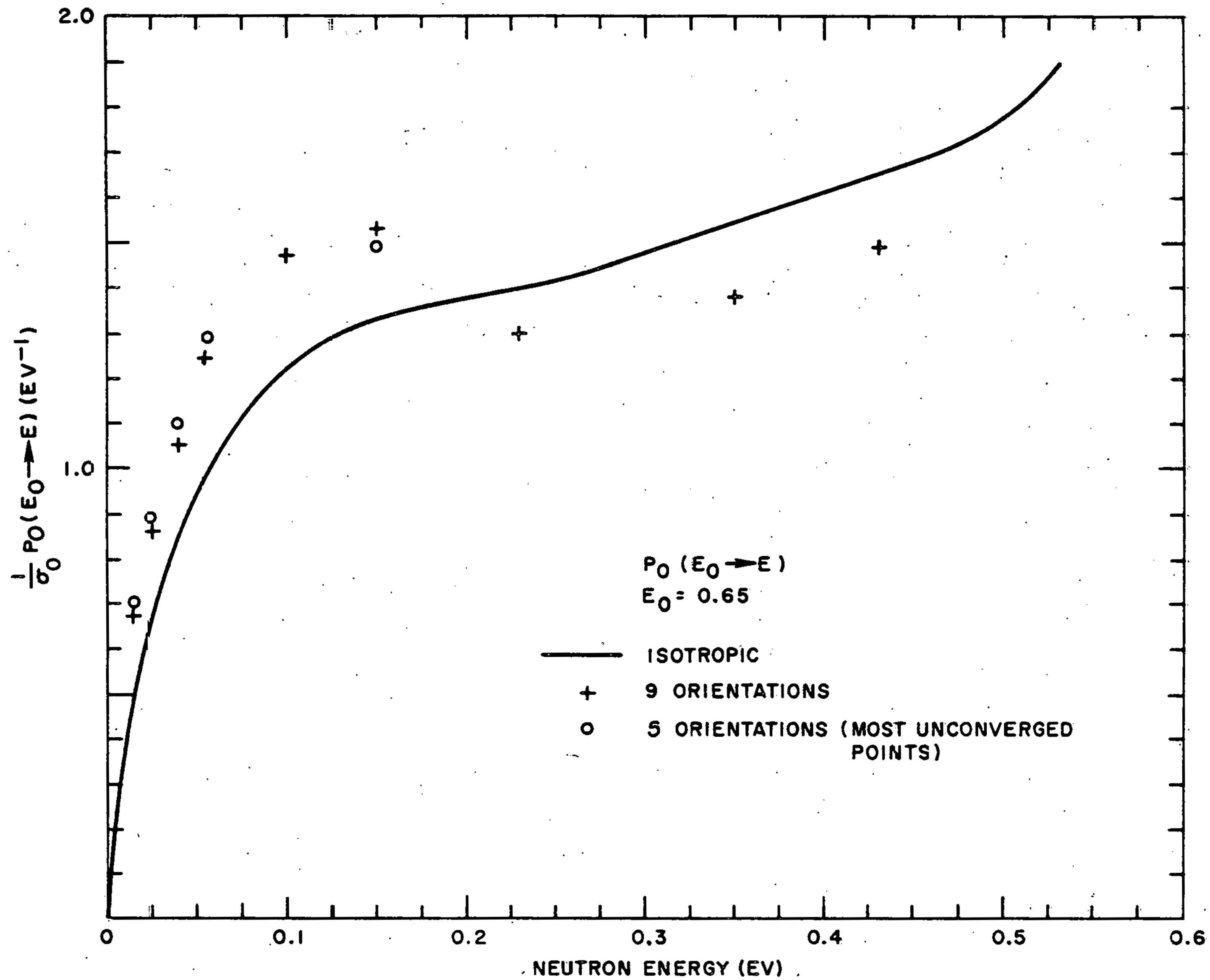

Fig. 16--Comparison of isotropic and anisotropic model for neutron scattering by water: $P_o(E_o \rightarrow E)$ at $E_o = 0.65$ ev

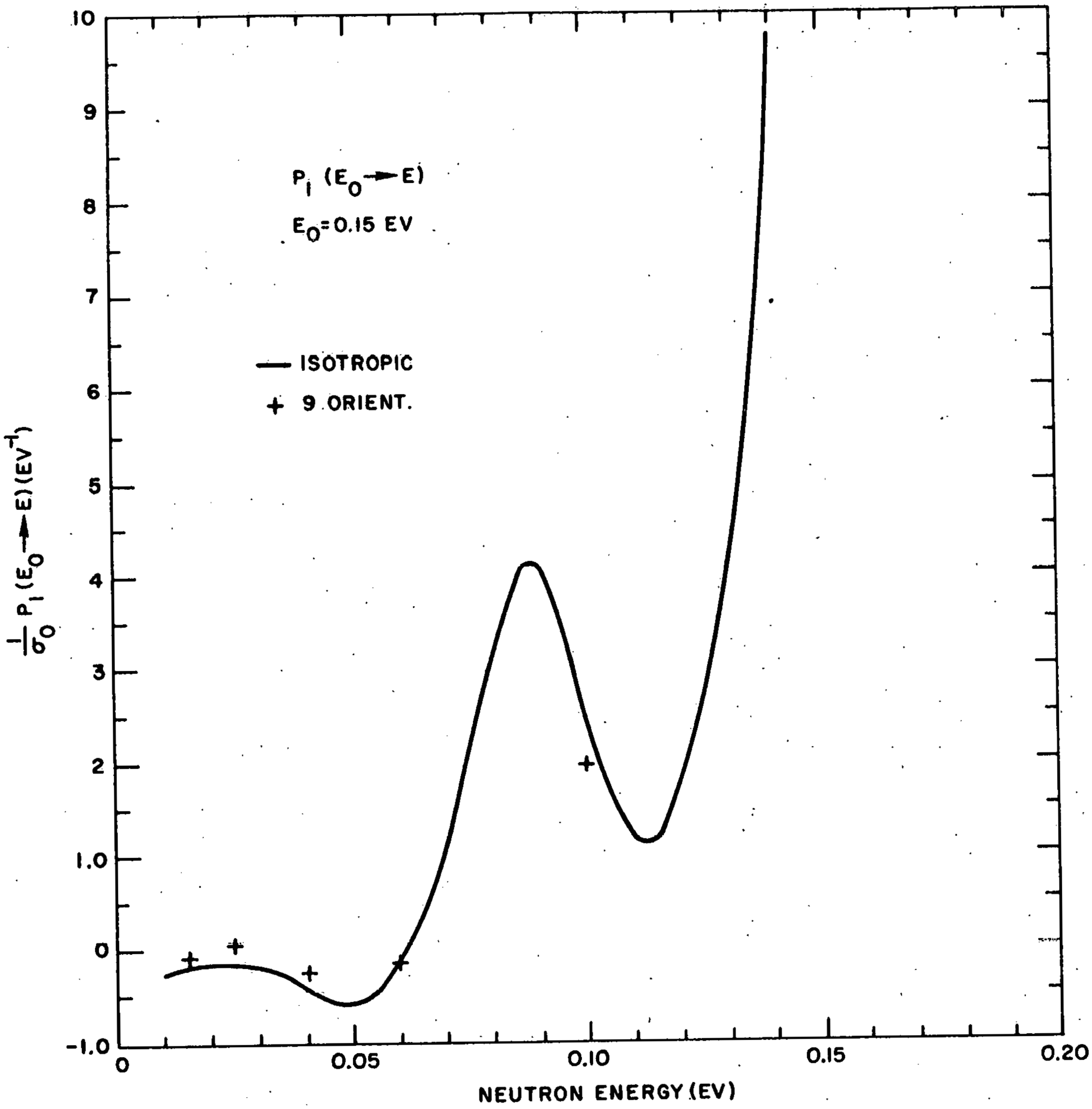

Fig. 17--Comparison of isotropic and anisotropic model for neutron scattering by water: $P_1(E_o \rightarrow E)$ at $E_o = 0.15$ ev

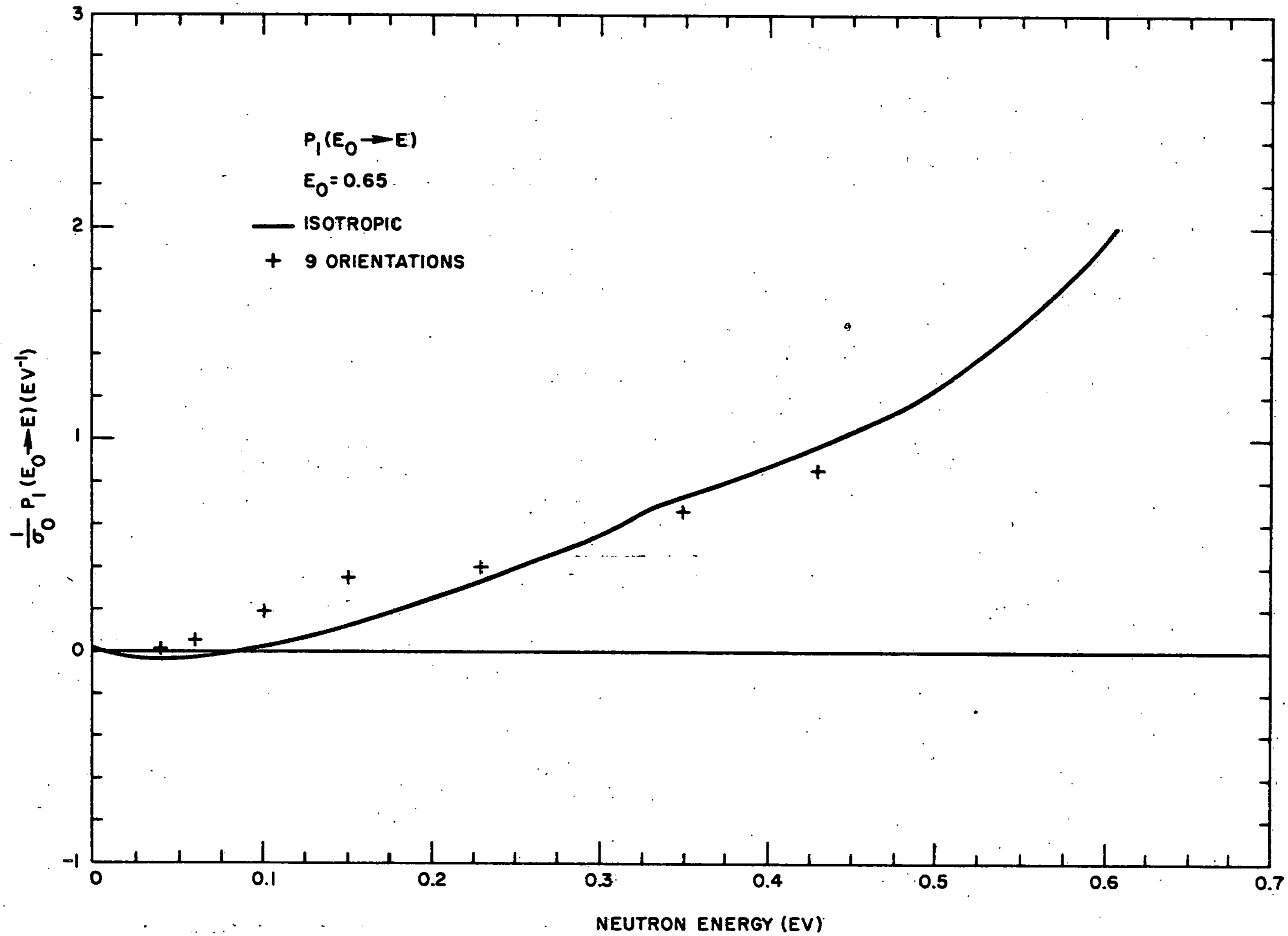

Fig. 18--Comparison of isotropic and anisotropic model for neutron scattering by water: $P_1(E_o \rightarrow E)$ at $E_o = 0.65$ ev

anisotropic model (11 energies). For low energies the average over orientation appeared to be well converged with only 5 orientations. For higher energies complete convergence was not achieved even with 9 orientations, although the trend of the difference between models was quite evident.

Another modification of GAKER under study is a more accurate integration over angles for the calculation of the $P_n(E \rightarrow E')$ matrices. In fact the 0 phonon term of the Nelkin model double differential cross section for H_2O has a singularity at $\begin{cases} \mu = 1 \\ E = E' \end{cases}$ which might impair the accuracy of numerical integration over angles. This term has the form

$$F(\alpha) = C\sqrt{\frac{\epsilon'}{\epsilon}} \; \frac{1}{\sqrt{\alpha}} e^{-a\alpha} \, I_o(b\alpha) \, \exp\left[- \frac{1}{4\alpha} (\epsilon' - \epsilon + \alpha)^2 \right]$$

with $\alpha = (\epsilon + \epsilon' - 2\mu \sqrt{\epsilon\epsilon'}) \frac{m}{M}$; $\epsilon = \frac{E}{kT}$; $\epsilon' = \frac{E'}{kT}$

The singularity at $\alpha \rightarrow 0$ (i.e., at $\mu \rightarrow 1$, $\epsilon' \rightarrow \epsilon$) is thus described by

$$f(\alpha) = \frac{1}{\sqrt{\alpha}} \exp\left[- \frac{1}{4\alpha} (\epsilon' - \epsilon + \alpha)^2 - a\alpha\right]$$

which can be integrated analytically to give

$$\int_{-1}^{1} f\left[\alpha(\mu)\right] \, d\mu = 4 \, \frac{M}{m} \, \frac{1}{\sqrt{\epsilon\epsilon'}} \int_{-y_{min}}^{y_{max}} dy \, \exp\left[- \frac{1}{4} (y + \frac{\gamma}{y})^2 - ay^2\right]$$

with $y = \sqrt{\alpha}$ and $\gamma = \epsilon' - \epsilon$

It is found that

$$\int_{-1}^{1} f(\alpha)\, d\mu = \frac{C'}{\sqrt{\eta\epsilon\epsilon'}} \exp\left[\gamma(\sqrt{\eta} - \tfrac{1}{2})\right] \frac{\sqrt{\pi}}{2} \left[\mathrm{erf}\,(z_{max}) - \mathrm{erf}\,(z_{min})\right]$$

$$+ \frac{C'}{\sqrt{\eta\epsilon\epsilon'}} \exp\left[-\gamma(\sqrt{\eta} + \tfrac{1}{2})\right] \frac{\sqrt{\pi}}{2} \,\mathrm{erf}\left[(x_{max}) - \mathrm{erf}\,(x_{min})\right]$$

where $\eta = \alpha + \frac{1}{4}$; $\quad C' = 2\frac{M}{m}$; $\quad y_{\substack{min\\max}} = \left|\sqrt{\epsilon} \pm \sqrt{\epsilon}\right|$

and $\quad z = y \quad \eta + \frac{\gamma}{2y}$

$\quad\quad x = y \quad \eta - \frac{\gamma}{2y}$

Hence, in order to integrate numerically over the singularity one writes

$$F(\alpha) = C\sqrt{\frac{\epsilon'}{\epsilon}} \left\{\left[e^{-\ \alpha} I_o(b\alpha) - 1\right] \exp -\left[\frac{1}{4\alpha}(\epsilon + \epsilon + \alpha)^2\right] + f(\alpha)\right\}$$

The first term in the bracket will be regular at $\alpha \to 0$ and the integral over the second is given by the preceding formulae.

4.4 UNIVERSAL SCATTERING CODE

At the present time there are a variety of computer codes available which are applicable for computing the scattering kernels of specific moderators, and thus the reactor physicist is able to make calculations on the moderator of his choice by choosing the appropriate code or combination of codes. It would, however, be very desirable to have a computer code which is applicable to all of the important reactor moderators, and which is simple to use. The usefulness of such a code from the practical standpoint is obvious.

The formulation of a general code to calculate the scattering kernel of all the important moderators has begun, and work on this project will continue in the next quarter.

V. GENERAL ATOMIC LINAC FACILITY STATUS

During the last nine months many improvements have been made in the General Atomic Linac facility to increase the reliability of the machine, upgrade its performance, and expand the utility of the experimental areas. Some major changes are underway and others are anticipated in the not too distant future. In this section a short summary of these changes will be given.

Over-all Linac performance has in general been quite good. Klystron lifetimes of 4000 to 6000 plate hours are common. Thyratron troubles in the modulators have been very annoying because of quality control failures attributed directly to the thyratron manufacturer. A change of thyratron type and manufacturer solved this problem and also simplified maintenance of this equipment. Modulator pulse lines have all been strengthened in a redesign of the modulators, and ease of tuning has been increased. Vac-ion pumps are being installed slowly throughout the Linac to eliminate all oil diffusion pumping equipment. The Linac has performed at or above its rated power output requirements on demand, going close to 2 amps of current at greater than 30 Mev electron energy for short pulses and to nearly 15 kw of average power for long pulse work.

The next major improvement anticipated for the Linac facility involves the relocation and upgrading of each modulator klystron microwave power source. Before the modulators are upgraded to utilize nominally 20 Mw klystrons, each modulator will be moved into a new building now under construction adjacent to the present accelerator building. All modulators will be located eventually in the new building, freeing badly needed experimental space in the accelerator room. The changes in the r.f. power system at the Linac are designed to increase the peak beam power of the Linac by a factor of four above that now normally in use for most neutron experiments. On the basis of our recent energy dependent yield measurement curves, neutron yields will probably be increased by a factor of 6 to 8. Since these changes must be made with no extended equipment shutdown time, the transition will probably take over a year to accomplish.

One further facility change being planned this year is the increase in the compartmentalization of the experimental areas to permit setup in one area while experiments proceed in adjacent areas. We are essentially attempting to divide the facility into four separate independent irradiation cells with appropriate shielding, beam stoppers, interlocks, radiation alarms, etc., to provide the necessary safety of operation.

An improvement in the Linac injection system is long overdue, since, as all L-band Linac owners know, the machine will accelerate much more current at short pulses than the present guns provide. An improved replacement gun or injection system is being looked into for the Linac, but at present no obvious simple approaches are on the horizon.

REFERENCES

1. Young, J. C., et al., Development of Multiplying Assembly, General Atomic Report, GA-2471, June 30, 1961.

2. Garelis, Edward and John L. Russell, Jr., Transactions of American Nuclear Society Meeting, Salt Lake City, Vol. 6, No. 1, p. 57 (1963).

3. Young, J. C., et al., Integral Neutron Thermalization, General Atomic Report, GA-4176, April 15, 1963.

4. Beyster, J. R., et al., Integral Neutron Thermalization, General Atomic Report, GA-3542, January 7, 1963.

5. Batchelor, R., et al., Nuclear Inst. and Methods 8, 146 (1960).

6. Batchelor, R., et al., Nuclear Inst. and Methods 13, 70 (1961).

7. Schmunk, R. E., et al., Phys. Rev. 128, 562 (1962).

8. Bell, Joan, SUMMIT, An IBM-7090 Program for the Computation of Crystalline Scattering Kernels, General Atomic Report, GA-2442, February 1, 1962.

APPENDIX

NEUTRON SPECTRA DATA BOOK FORMAT

The presentation of experimental and theoretical data concerning neutron spectra has previously been troublesome and cumbersome. It is hoped that the format set forth in this appendix will initiate a procedure for displaying data in a standard form such that sufficient information is given for inter-comparisons of data and calculations between this and other laboratories. It should be pointed out that this format is of a typical experiment performed at General Atomic previously but could be expanded to include all "best data" available. A compilation of this sort should be a highly valuable and use-ful tool for all reactor physicists, and an effort to get this work under way will be made.

The geometrical arrangement and information necessary to calculate the resulting spectrum, and the experimental results in comparison to the most recent theoretical models used to describe the data are shown in the following two pages.

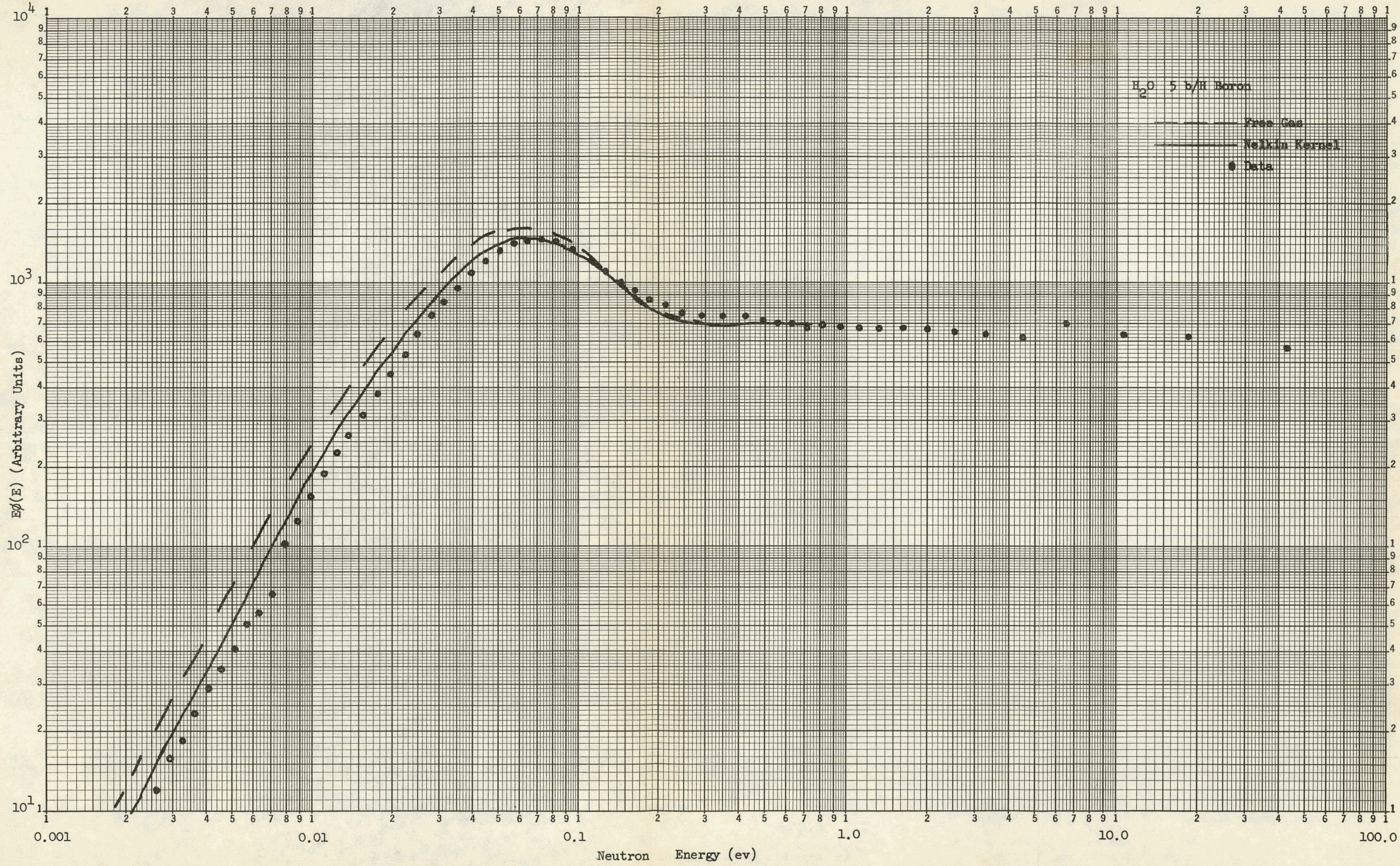
H_2O 5 b/H Boron
Free Gas
Nelkin Kernel
Data
EØ(E) (Arbitrary Units)
Neutron Energy (ev)
0.001
0.01
0.1
1.0
10.0
100.0

INFINITE MEDIUM NEUTRON SPECTRUM IN BORATED H_2O

CALCULATION PARAMETERS

Kernel: Nelkin Water (ID 43700) and Free Gas (ID 40205)

Code: SPECTRUM

Temperature: 0.0255 ev

Source: erf $\sqrt{E/KT_{eff}}$ (KT_{eff} 0.117 ev)

ATOM DENSITIES x 10^{-24}

$N_H = 0.0666$

$N_B = 0.000427$

LOCAL BUCKLING

$B^2_{transverse} = 0.02\ cm^{-2}$

$B^2_{axial} = 0$

$\left(\frac{\text{total absorptions}}{\text{slowing down density}}\right) = 1.002$

COMMENTS:

Spatial Effects Negligible

EXPERIMENTAL ARRANGEMENT

PLAN VIEW

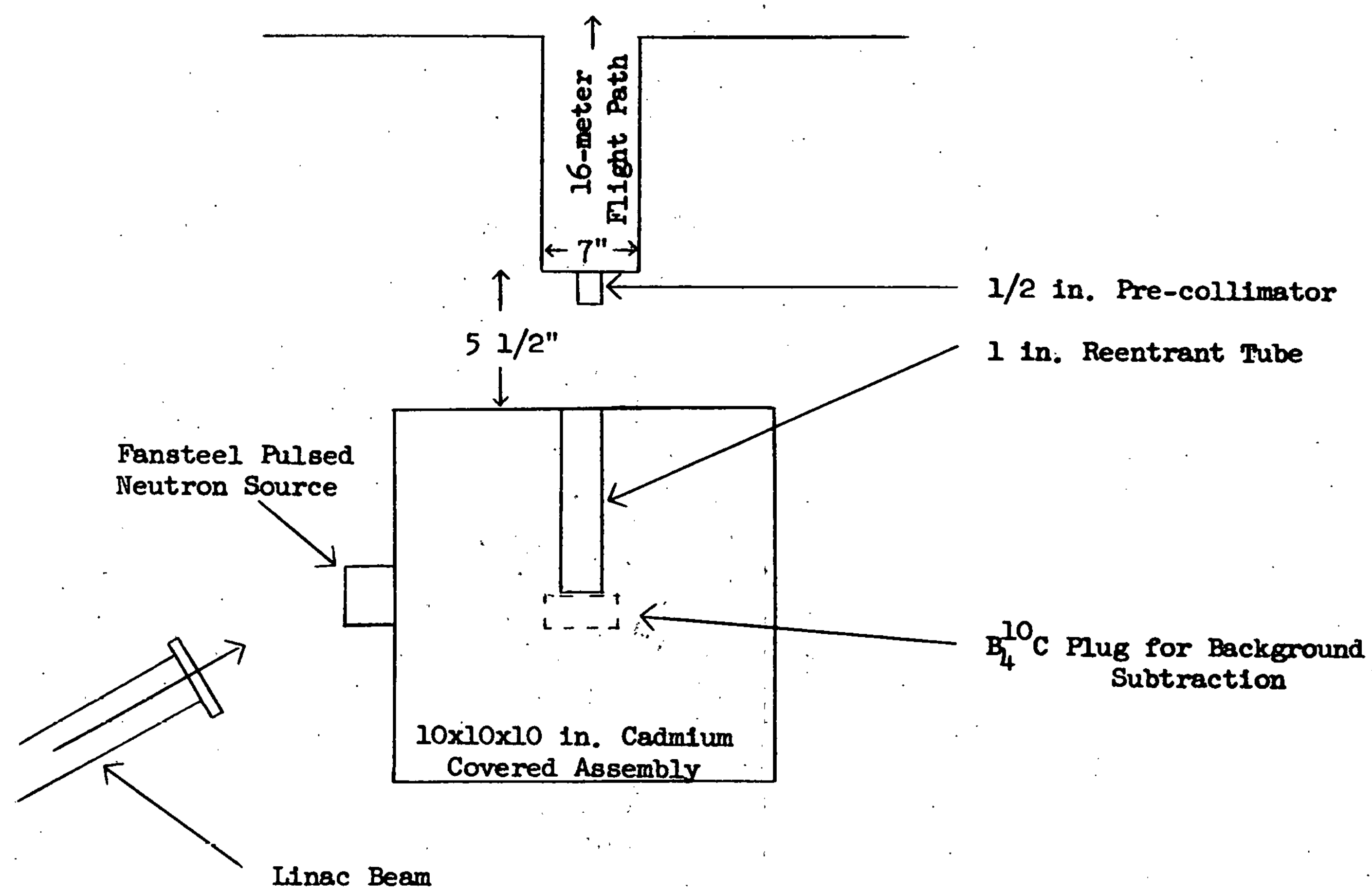

NOT TO SCALE